Side-Bonded Pd-η^2-$(C_2H_2)_{1,2}$ and Pd_2-η^2-(C_2H_2) Complexes: Infrared Spectra and Density Functional Calculations

Xuefeng Wang and Lester Andrews*

Department of Chemistry, University of Virginia, Charlottesville, Virginia 22904-4319

Received: August 12, 2002; In Final Form: November 14, 2002

Laser-ablated palladium atoms react with acetylene in excess argon to form the strong Pd-η^2-(C_2H_2) and Pd-η^2-$(C_2H_2)_2$ π complexes. The C−C and C−H stretching modes and two C−H deformation modes are observed in the matrix infrared spectrum and identified through isotopic substitution ($^{13}C_2H_2$, C_2D_2, C_2HD) and density functional theory (DFT) isotopic frequency calculations. The Pd(C_2H_2) complex is characterized by a C−C stretching mode near 1710 cm^{-1} and a 39.8 kcal/mol binding energy predicted by DFT. The antisymmetric C−C stretching mode for Pd-η^2-$(C_2H_2)_2$ is observed at 1765 cm^{-1}. The Pd_2-η^2-(C_2H_2) complex produced from the reaction of two Pd atoms with C_2H_2 is characterized by a C−C mode at 1566 cm^{-1}. The interaction between atomic Pd and C_2H_2 involves a small amount of charge transfer based on NBO analysis, which is enhanced by a Pd_2 dimer coordinated to C_2H_2. As a result, Pd_2 dimer can reduce the C−C triple bond to a double bond. These complexes represent first steps in the Pd−C_2H_2 interaction culminating in acetylene chemisorbed on palladium.

Introduction

The complexes of a bare transition metal atom with molecular hydrogen, carbon monoxide, and hydrocarbons are fundamentally important in studying bond activation, catalysis, and chemisorption. Accordingly, palladium chemistry is a rich avenue for investigation.[1−3] Transition metal atom and cation reactions with ethane, ethylene, propane, and propylene have been studied extensively using photoionization mass spectrometry (PIMS).[4] More recently, the side-bonded palladium−hydrogen complexes $Pd(H_2)_{1,2,3}$ have been synthesized in solid argon and neon, which established a simple model for hydrogen activation and oxidative addition reactions.[5] Palladium and its clusters[6−9] are of particular interest for applications in heterogeneous catalysis where experimental observation and theoretical calculation have advanced the understanding of active surface species.[10−13] These works show that on Pd(111) below 200 K, the adsorbed species is molecular acetylene, but at higher temperatures, typically above 250 K, adsorbed acetylene transforms into vinylidene, which is an intermediate in hydrogenation reactions.[13] Likewise, vibrational frequency measurements and calculations have characterized new transition metal dihydrogen complexes and hydride intermediate species. Complexes such as $(H_2)AuH$, $(H_2)RhH_2$, and $(H_2)LaH_2$ and hydrides such as PtH_2 and WH_6 have been observed recently by matrix infrared spectroscopy.[14−16]

Metal atom reactions with acetylene give a wide range of products depending on the metal. Lithium forms the π complex $Li(C_2H_2)$,[17] and sodium forms the vinylidene $NaCCH_2$ complex,[18] but the HBeCCH insertion product[19] and MCCH (M = Be, Mg, Ca, Sr) decomposition products are produced with group 2 metals.[19,20] Additional $M(C_2H_2)$ complexes are obtained in the reactions of group 13 metals with C_2H_2, but boron also forms the HBCCH insertion product, and on photolysis, Al(C_2H_2) rearranges to HAlCCH.[21] In contrast, transition metal atom reactions with acetylene have been investigated less extensively. Early thermal Fe and Ni atom reactions with C_2H_2 gave the HFeCCH insertion and Ni(C_2H_2) complex products in matrix infrared spectroscopy studies.[22,23] Because of the wide range of possible chemical products, it is desirable to explore further the chemistry of reactions of transition metals and C_2H_2 and to find new routes for the activation of stable bonds and the formation of different products.

The interaction of acetylene and transition metals has been investigated more traditionally in solution with complex ions. Infrared spectra of Pt(II) complexes with alkynes show a 200 cm^{-1} reduction in the C≡C stretching vibration.[24] This work has been extended to $L_2Ni(II)$ and $L_2Pd(II)$ complexes of substituted alkynes, and the reductions in C≡C frequency are less than that for $L_2Pt(II)$ complexes.[25] Chatt et al. suggested that the bonding to acetylene can be described as (i) donation of acetylene π electron density into an empty p or d orbital on the metal and back donation of electron density from a filled metal d orbital to an acetylene π^* orbital or (ii) reorganization of electrons to give an olefin with two σ carbon−metal bonds in a metallacyclopropene ring.[26]

We report here reactions of laser-ablated Pd atoms with C_2H_2 in excess argon. A series of novel complexes, Pd-η^2-$(C_2H_2)_{1,2}$ and Pd_2-η^2-(C_2H_2), are characterized through matrix infrared spectra. The vibrational frequencies are confirmed by isotopic substitution and density functional theory (DFT) structure, frequency, and infrared intensity calculations. It is noteworthy that two Pd atoms (Pd_2 dimer) elongate the C−C bond to 1.312 Å in Pd_2-η^2-(C_2H_2) as compared to the 1.269 Å C−C bond in Pd-η^2-(C_2H_2) and the 1.336 Å C−C bond in C_2H_4, based on DFT structures.

Experimental and Theoretical Methods

The experimental methods employed for reacting laser-ablated transition metal atoms with small molecules and for identifying the reaction products from matrix infrared spectra have been described previously,[27] and the same methods were applied here

* To whom correspondence should be addressed. E-mail: lsa@virginia.edu.

10.1021/jp0267454 CCC: $25.00
Published on Web 12/24/2002

for the reaction of palladium with C_2H_2. The Nd:YAG laser fundamental (1064 nm, 10 Hz repetition rate with 10 ns pulse width) was focused onto the rotating palladium target (Alfa Aesar, foil, 99.95%). Laser-ablated metal atoms were codeposited with 0.1−0.6% C_2H_2 ($^{13}C_2H_2$, C_2D_2, or mixed C_2H_2, C_2HD, C_2D_2) in excess argon onto a 7 K or neon onto a 4 K CsI cryogenic window at 2−4 mmol/h for 1 h. Infrared spectra were recorded at 0.5 cm^{-1} resolution on a Nicolet 750 with 0.1 cm^{-1} accuracy using a liquid N_2-cooled HgCdTe detector. Matrix samples were subjected to UV−vis irradiation from a medium pressure mercury arc lamp.

DFT frequency calculations were performed to reproduce the structures and frequencies of palladium−acetylene complexes using the Gaussian 98 program.[28] Both BPW91 and B3LYP density functionals[29,30] with 6-311++G(d,p) basis sets for C and H atoms and the SDD pseudopotential for the Pd atom were employed.[31,32] Geometries were fully optimized, and the vibrational frequencies were calculated analytically from second derivatives. Natural bond orbital analysis[33] was done to determine the electron configurations and natural charge distributions.

Results

Infrared Spectra. Infrared spectra of laser-ablated Pd atom reactions with C_2H_2 in excess argon at 7 K are presented in Figures 1−3, and the product absorptions are listed in Table 1. Absorptions common in laser-ablated metal experiments with acetylene,[34] namely, CCH (1846.1, 2103.5 cm^{-1}), CCH^+ (1820.2 cm^{-1}), CCH^- (1770.5 cm^{-1}), C_4H (2060.4 cm^{-1}), C_4H_2 (3225.4, 627.7 cm^{-1}), and $C_2H_2^+$ (3104.5 cm^{-1}), have been reported previously.[34−38] These bands have also been observed in argon discharge experiments with acetylene and in other investigations of hydrocarbon transients.[34−37] In addition, CH_2CO (2142.0 cm^{-1}), C_4 (1543.3 cm^{-1}), PdNN (2209.7 cm^{-1}), and PdCO (2044.0 cm^{-1}) are observed,[39−42] and C_2H_4 (947.4 cm^{-1}) and C_2H_3 (900 cm^{-1}) are detected on deposition.[43,44] Additional bands common to other metal experiments with C_2H_2 are listed as C_xH_y in Table 1. Strong diatomic PdH (1952.8 cm^{-1}) and PdD (1403.5 cm^{-1}) absorptions, also found in laser-ablated Pd atom experiments with H_2 and D_2,[5] are observed in Pd reactions with C_2H_2 and C_2D_2. The dihydrogen complex, $Pd(H_2)$ (953.8, 949.4 cm^{-1}), is also present in these experiments, but it only appeared on annealing suggesting the combination of PdH and H atom in solid argon.[5]

Two different concentrations of C_2H_2 (0.2 and 0.5%) are employed for the reactions of Pd with C_2H_2 on cocondensation with argon, and three groups of absorptions are unique as new reaction products. Group A bands at 3163.8, 3153.7, 1716.9, 1709.6, 1707.1, 769.6, 765.8, 764.5, 675.4, and 674.5 cm^{-1} appeared on deposition, increased by 60% on annealing to 30 K, decreased by 20% on broadband photolysis, and increased again on further annealing to 35 K and are labeled PdA (Figure 1). This group is favored in the experiments with dilute C_2H_2 concentration (0.2%). Group B bands at 3184.2, 1765.3, 1762.9, 1760.4, 772.8, and 710.1 cm^{-1} are favored at higher C_2H_2 concentrations and are labeled PdA_2. Group B is observed on deposition in 0.5% C_2H_2 but barely appeared with 0.2% C_2H_2 and increased stepwise on annealing and photolysis afterward. Group C bands at 1572.3, 1565.8, 989.6, and 985.7 cm^{-1} are weak on initial deposition, increase on annealing, decrease on photolysis, and are favored at higher laser energy, which produces a higher Pd atom concentration, and are labeled Pd_2A.

Carbon-13 and deuterium isotopic counterparts of new product absorptions are also listed in Table 1. Spectra using mixed $^{12}C_2H_2$ and $^{13}C_2H_2$ and mixed C_2H_2, C_2HD, and C_2D_2 samples are recorded to help identify the molecular stoichiometries. Figures 2 and 3 show C_2D_2 and mixed H/D spectra.

TABLE 1: Infrared Absorptions (cm^{-1}) Observed for Pd + C_2H_2 Reaction Products in Solid Argon at 7 K

$^{12}C_2H_2$	$^{12}C_2H_2 + {}^{13}C_2H_2$	$^{13}C_2H_2$	C_2D_2	assignment
3326.0	3326.0, 3324.6, 3309.7, 3308.8	3308.8	2593.4	C_4H_2
3184.2		3178.2	2373.5	$Pd(C_2H_2)_2$
3163.8		3157.7	2363.6	$Pd(C_2H_2)$
3153.7		3147.4	2360.2	$Pd(C_2H_2)$
3104.5	3104.5, 3095.0	3095.0	2311.5	$C_2H_2^+$
2084.0		2006	2056	C_xH_y
2060.4	2060.4, 2029.8, 2017.9, 1981.5	1981.5	2049.4	C_4H
2142.0		2080.0	2112.4	CH_2CO
2104		2053	1971	CCH
1987.7		1916.3	1856.3	PdCCH
1952.8	1952.8	1952.8	1403.5	PdH
1899.0		1830.9	1800.0	$PdCCH^-$
1878.0		1810.6	1780.9	$[PdCCH^-]X$
1845.8	1845.8, 1785.5	1785.5	1746.5	CCH
1820.4		1754.8	1724.6	CCH^+
1770.5	1770.5, 1711.8	1711.8	1676.7	CCH^-
1765.3	1765.3	1706.1[a]		$Pd(C_2H_2)_2$
1762.9		1704.2	1618.7	$Pd(C_2H_2)_2$
1760.4	1760.9, 1701.3	1701.2	1617.9	$Pd(C_2H_2)_2$
1716.9	1716.9, 1659.1	1659.1[a]	1590.4	$Pd(C_2H_2)$
1709.6	1709.6, 1652.7	1651.8[a]	1582.8	$Pd(C_2H_2)$
1707.1	1707.1, 1649.5	1649.5[a]	1579.4	$Pd(C_2H_2)$
1660.9	1660.9, 1601.6	1601.6	1539.8	$[Pd(C_2H_2)]X$
1572.3	1572.3, 1521.2	1521.4	1506.4	$Pd_2(C_2H_2)$
1565.8	1565.8, 1515.6	1515.6	1500.7	$Pd_2(C_2H_2)$
1543.3		1483.6	1543.3	C_4
989.6		975.5	846.3	$Pd_2(C_2H_2)$
985.7		971.6	844.7	$Pd_2(C_2H_2)$
977.7		975.0		C_xH_y
971.2		968.2		C_xH_y
926.5		916.8		C_xH_y
900.4		897		C_2H_3
893.5		887.5		C_xH_y
855.5		847.9		C_xH_y
853.1		845.2		C_xH_y
772.8		766.3	638.7	$Pd(C_2H_2)_2$
769.6		764.7		$Pd(C_2H_2)$
765.8		757.3	636.7	$Pd(C_2H_2)$
764.5		756.1	635.7	$Pd(C_2H_2)$
710.1		706.2	513.6	$Pd(C_2H_2)_2$
675.4	675.4, 672.3	672.3	508.1	$Pd(C_2H_2)$
674.5	674.5, 671.5	671.5	506.7	$Pd(C_2H_2)$
627.7	627.3, 622.8	622.4	495.6	C_4H_2
615.3		609.8	482.4	C_4H?
600.5	600.5, 597.1	597.1		$Pd_xC_yH_z$
595.7	595.7, 590.8	590.8	475.8	$Pd_xC_yH_z$

[a] Absorptions for $Pd(^{12}C^{13}CH_2)(^{12}C_2H_2)$ are 1738.7 cm^{-1} and for $Pd(^{12}C^{13}CH_2)$ are 1687.6, 1681.0, and 1678.6 cm^{-1} from 2% $^{12}C^{13}CH_2$ present in the $^{13}C_2H_2$ sample.

Infrared spectra of analogous reaction products in excess neon at 4 K are shown in Figure 4, and the isotopic product absorptions are given in Table 2. Small shifts between neon and argon are characteristic of a weak matrix interaction. The metal independent bands have been identified by earlier workers.[33,36]

Calculations. DFT calculations predict the geometries and frequencies (intensities) of Pd-η^2-$(C_2H_2)_{1,2}$ and $Pd_{2,3}$-η^2-(C_2H_2) in several isomeric forms, and the results are summarized in Tables 3 and 4. We find the complex of Pd with C_2H_2, Pd-η^2-(C_2H_2) ($^1A_1$) with C_{2v} symmetry, to be energetically favorable where the C−C and C−H bonds are elongated by 0.06 and 0.01 Å, respectively, as compared with free C_2H_2 using BPW91 calculations. The singlet PdCHCH species converged to Pd-η^2-(C_2H_2). In addition, the vinylidene form, $PdCCH_2$, is

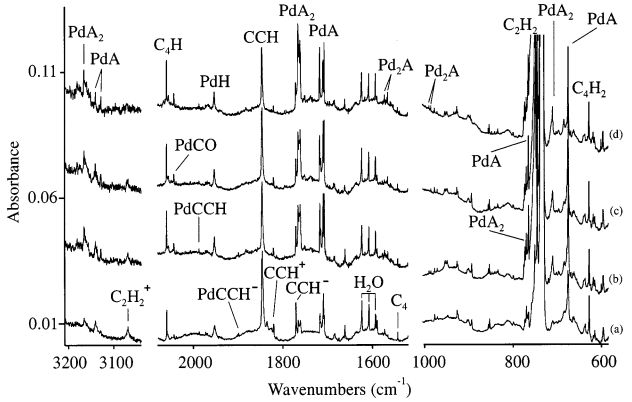

Figure 1. Infrared spectra of the products formed by reactions of laser-ablated Pd and C_2H_2 in excess argon codeposited at 7 K. (a) C_2H_2 (0.5%) in argon deposited for 60 min, (b) after annealing to 30 K, (c) after $\lambda > 240$ nm irradiation for 20 min, and (d) after annealing to 35 K.

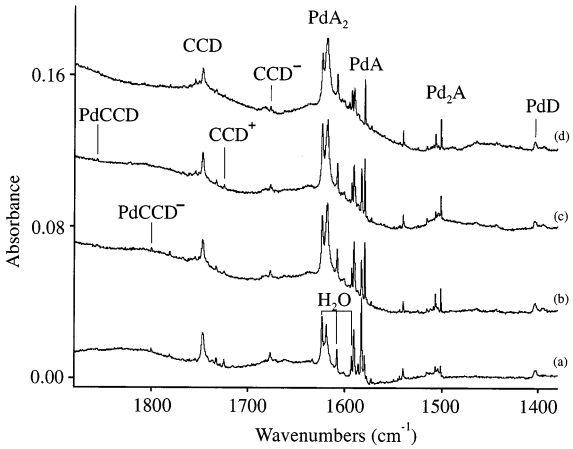

Figure 2. Infrared spectra of the products formed by reactions of laser-ablated Pd and C_2D_2 in excess argon codeposited at 7 K. (a) C_2D_2 (0.5%) in argon deposited for 60 min, (b) after annealing to 30 K, (c) after $\lambda > 240$ nm irradiation for 20 min, and (d) after annealing to 35 K.

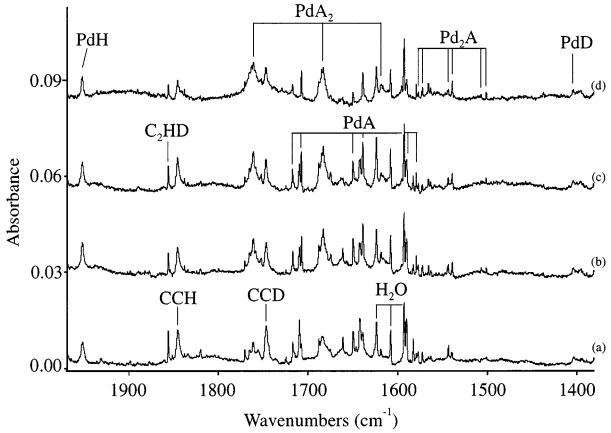

Figure 3. Infrared spectra of the products formed by reactions of laser-ablated Pd and a C_2H_2, C_2HD, C_2D_2 mixture (30, 50, 20%) in excess argon codeposited at 7 K. (a) Acetylene (0.6%) in argon deposited for 60 min, (b) after annealing to 30 K, (c) after $\lambda > 240$ nm irradiation for 20 min, and (d) after annealing to 35 K.

9.9 kcal/mol higher, and the metal inserted isomers, H−Pd−CCH ($^1A'$) and ($^1\Sigma^+$), are higher in energy by 21.4 and 63.9 kcal/mol, respectively, which is not the case for the beryllium−acetylene and magnesium−acetylene systems, where the most stable form is the insertion product HMCCH ($^1\Sigma^+$).[19] Siegbahn concluded earlier that the C−H bond addition of Pd is unfavorable due to the stability of the molecular complex.[45]

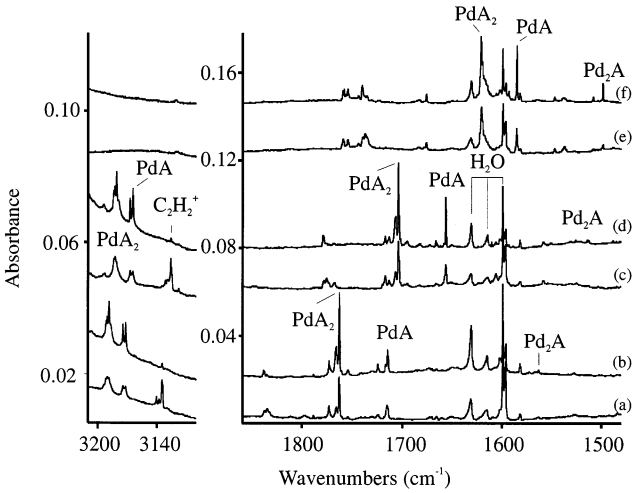

Figure 4. Infrared spectra of the products formed by reactions of laser-ablated Pd and C_2H_2 in excess neon codeposited at 4 K. (a) C_2H_2 (0.1%) in neon deposited for 60 min, (b) after annealing to 10 K; (c) $^{13}C_2H_2$ (0.2%) in neon deposited for 60 min, (d) after annealing to 10 K; and (e) C_2D_2 (0.2%) in neon deposited for 60 min and (f) after annealing to 10 K.

TABLE 2: Infrared Absorptions (cm^{-1}) Observed for Pd + C_2H_2 Reaction Products in Solid Neon at 4 K

C_2H_2	$^{13}C_2H_2$	C_2D_2	assignment
3191.7	3184.2	2369.2	$Pd(C_2H_2)_2$ (site)
3190.5	3182.8	2368.0	$Pd(C_2H_2)_2$
3188.6	3181.1	2366.3	$Pd(C_2H_2)_2$ (site)
3174.6	3167.5	2357.1	$Pd(C_2H_2)$ (site)
3171.7	3164.4	2355.0	$Pd(C_2H_2)$
3135	3125	2327	$C_2H_2^+$
2063.7	1984.7	2052.5	C_4H
1838.1	1778.7	1739.7	CCH
1835.2	1775.6	1737.2	CCH (site)
1832.2	1767.6	1735.1	CCH^+
1773.0	1717.0	1676.7	CCH^-
1765.8	1706.6		$Pd(C_2H_2)_2$ (site)
1762.9	1703.7	1620.9	$Pd(C_2H_2)_2$
1724.1	1666.3		$Pd(C_2H_2)$ (site)
1716.4	1658.2	1586.0	$Pd(C_2H_2)$ (site)
1714.6	1656.3	1585.0	$Pd(C_2H_2)$
1665.2	1605.9	1537.2	$[Pd(C_2H_2)]X$
1562.7	1513.7	1498.1	$Pd_2(C_2H_2)$
1280.7	1260.5	1115.7	?
713.6	709.6		$Pd(C_2H_2)_2$ (site)
712.3	708.6	515.2	$Pd(C_2H_2)_2$
678.4	675.9	508.8	$Pd(C_2H_2)$
676.8	674.1	507.2	$Pd(C_2H_2)$ (site)
630.8	624.4	497.2	C_4H_2

Analogous calculations for Pd-η^2-(C_2H_2) anion and cation complexes show little change in the structural parameters and small changes in frequencies. Previous cation calculations reveal stable side-bound electrostatic complexes.[46]

A similar complex is calculated with two C_2H_2 moieties associated with one Pd atom. The Pd-η^2-$(C_2H_2)_2$ molecular structure is converged to D_{2d} symmetry in the $^1A_1$ ground state, which is analogous to that found for $Pd(H_2)_2$.[5] The C−C bond is calculated to be 0.007 Å shorter (BPW91) than that in Pd-η^2-(C_2H_2), indicating that the interaction of Pd with each C_2H_2 subunit in Pd-η^2-$(C_2H_2)_2$ is slightly reduced. Calculations with the B3LYP functional give essentially the same results. Figure 5 illustrates structures calculated for these complexes. Several attempts to calculate a tris complex failed to converge.

TABLE 3: Geometries and Frequencies Calculated at the BPW91/6-311++G(d,p)/SDD Level of Theory for $Pd(C_2H_2)_{1,2}$ and $Pd_{2,3}(C_2H_2)$ Complexes

molecule	state	relative energy (kcal/mol)	geometries (Å, deg)	frequencies (cm^{-1}) (modes, intensities, km/mol)
C_2H_2	$^1\Sigma_g^+$		CC, 1.209; CH, 1.070	3463.2(σ_g, 0), 3363.9(σ_u, 84), 2005.4(σ_g, 0), 742.0(π_u, 109), 584.4(π_g, 0)
CCH_2 (C_{2v})	$^1A_1$	42.3	CC, 1.303; CH, 1.096; HCH, 118.4	3129.6(b_2, 24), 3053.6(a_1, 51), 1661.5(a_1, 99), 1160.1(a_1, 30), 699.7 (b_1, 98), 252.7(b_2, 4)
PdCCH ($C_{\infty v}$)	$^2\Sigma^+$	0.0	CC, 1.225; CH, 1.070; PdC, 1.904	3403.5(σ, 62), 2014.7(σ, 23), 530(π, 2 × 28), 470.2(σ, 5), 215.4(π, 16 × 2)
$PdCCH^+$	$^1\Sigma^+$	223	CC, 1.215; CH, 1.077; PdC, 1.857	3343.1(σ, 189), 2072.4(σ, 28), 788.2(π, 2 × 195), 528.2(σ, 0), 191.5(π, 2 × 9)
$PdCCH^-$ ($C_{\infty v}$)	$^1\Sigma^+$	−50.1	CC, 1.241; CH, 1.070; PdC, 1.890	3385.8(σ, 29), 1912.9(σ, 356), 433(π, 2 × 65), 403.6(σ, 143), 258(π, 2 × 14)
Pd-η^2-C_2H_2 (C_{2v})	$^1A_1$	0.0	PdC, 2.037; CC, 1.269; CH, 1.080; CPdC, 36.3; CCH, 154.8	3294.2(a_1, 3), 3231.5(b_2, 25), 1720.7(a_1, 18), 766.3(a_1, 0), 762.9(b_2, 85), 670.3(b_1, 80), 600.3(a_2, 0), 462.8(a_1, 6), 386.9(b_2, 5)
$PdCCH_2$ (C_{2v})	$^1A_1$	9.9	CC, 1.312; CH, 1.094; PdC, 1.812; HCH, 118.5	3133.9(b_2, 6), 3055.3(a_1, 33), 1678.6(a_1, 223), 1257.8(a_1, 2), 693.5(b_2, 19), 682.8(b_1, 86), 521.9(a_1, 1), 238.8(b_1, 34), 210.9(b_2, 32)
HPdCCH (C_s)	$^1A'$	21.4	CC, 1.225; CH, 1.070; PdC, 1.881; PdH, 1.517; HPdC, 77.3	3402.5(59), 2181.9(33), 2011.5(4), 596.0(67), 566.3(70), 500.8(3), 442.4(2), 245.8(17), 215.2(18)
HPdCCH ($C_{\infty v}$)	$^1\Sigma^+$	63.9	CC, 1.228; CH, 1.071; PdC, 2.031; PdH, 1.597	3388.8(σ, 40), 2001.6(σ, 6), 1880.7(σ, 539), 983.6(π, 225 × 2), 645.9(π, 89 × 2), 412.7(σ, 62), 190.1(π, 12 × 2)
Pd-η^2-$(C_2H_2)_2$ (D_{2d})	$^1A_1$		PdC, 2.067; CC, 1.262; CH, 1.079; CPdC, 35.6; CCH, 156.6	3307.4(b_2, 16), 3307.3(a_1, 0), 3242.6(e, 2 × 26), 1760.7(b_2, 106), 1746.3(a_1, 0), 755.5(b_2, 12), 752.8(a_1, 0), 750.9(e, 2 × 69), 713.3(e, 2 × 34), 677.6(b_1, 0), 668.0(a_2, 0), 468.0(e, 2 × 0), 457.5(b_2, 19), 409.8(a_1, 0), 228.0(b_1, 0), 111.1(e, 2 × 3)
parallel Pd_2-η^2-C_2H_2 (C_{2v})	$^1A_1$	0.0	PdC, 1.950; CC, 1.312; CH, 1.905; PdPd, 2.582; CPdPd, 71.0; PdCH, 116.3	3098.1(a_1, 0), 3062.2(b_2, 0), 1563.6(a_1, 48), 986.6(b_2, 39), 860.8(a_1, 17), 603.6(a_2, 0), 581.2(b_1, 77), 562.7(a_1, 0), 559.0(b_2, 0), 270.7(b_2, 0), 191.8(a_2, 0), 182.6(a_1, 0)
$(Pd)_2CCH_2$ (C_{2v})	$^1A_1$	−1.4	PdPd, 2.583; PdC, 1.921; CC, 1.331; CH, 1.095; HCH, 117.5	3116.5(b_2, 0), 3039.3(a_1, 0), 1592.4(a_1, 120), 1307.3(a_1, 0), 884.8(b_2, 0), 719.2(b_1, 68), 535.5(b_2, 4), 472.1(a_1, 0),.... 180.3(a_1, 0)
perpendicular Pd_2-η^2-C_2H_2 (C_{2v})	$^1A_1$	5.0	PdC, 2.060; CC, 1.335; CH, 1.086; PdPd, 2.804; CPdC, 37.8; CCH, 145.9	3193.1(a_1, 1), 3153.7(b_2, 9), 1465.9(a_1, 11), 832.2(b_2, 97), 781.9(a_1, 1), 718.3(b_1, 7), 677.8(a_2, 0), 427.4(b_1, 4), 426.6(b_2, 11), 425.3(a_1, 4), 263.0(a_2, 0), 116.5(a_1)
$(Pd_3)CCH_2$	$^1A_1$	0.0	PdC, 1.959, 1.980; PdPd, 2.683, 2.757; CC, 1.361; CH, 1.094; PdCC, 125.8, 131.2	3133.9(a′, 0), 3048.0(a′, 0), 1467.3(a′, 85), 1298.5(a′, 2), 902.5(a′, 0), 685.0(a″, 67),...
ring Pd_3-η^2-C_2H_2 (C_{2v})	$^1A_1$	20.3	Pd′C, 1.921; CC, 1.320; CH, 1.104; Pd′Pd″, 2.537; Pd′Pd″Pd′, 88.6; Pd′CC, 125.4; CCH, 127.0	2998.9(a_1,3), 2966.8(b_2,2), 1566.1(a_1,56), 1042.1(b_2,7), 891.6(a_1,22), 563.3(a_2,0), 550.5(b_2,3), 534.5(b_1,83), 517.6(a_1,0), 335.7(b_2,1), 196.6(a_1,0), 194.7(b_2,0), 188.9(a_2,0), 77.6(a_1,0), 40.3(b_1,0)
(CH)−Pd_3−(CH) (D_{3h})	$^1A_1$	40.3	PdC, 1.988; CC, 2.216; CH, 1.102; PdPd, 2.858; CPdC, 67.7; CCH, 180.	3000.1(0), 2993.8(0), 856.7(1), 856.3(1), 669.1(0), 645.1(0), 644.6(0), 519.6(0), 518.8(0), 511.6(30), 432.4(0), 431.5(0), 201.8(0), 111.8(0), 110.6(0)

When two Pd atoms coordinate C_2H_2, two side-bonded structure isomers are obtained, namely, parallel and perpendicular Pd_2-η^2-(C_2H_2), in which the Pd−Pd subunit retains its metal−metal bond. For parallel Pd_2-η^2-(C_2H_2) with a parallelogram structure, the C−C bond is calculated to be 1.312 Å long (BPW91), which is very close to the 1.336 Å C−C bond length for free C_2H_4 calculated at the same level and indicates that the triple C−C bond is reduced to a double C−C bond. This structure is similar to chemisorbed acetylene.[10] It is interesting to note that the Pd−C bond length is 1.950 Å, approximately the same as this bond length in the Pd−CCH molecule, suggesting a strong chemical interaction. The other isomer, perpendicular Pd_2-η^2-(C_2H_2), lies 5.0 kcal/mol higher in energy, where each Pd atom interacts with two carbon atoms and the C−C bond is further weakened to 1.335 Å. However, the bridge-bonded $(Pd_2)CCH_2$ vinylidene is the most stable isomer. The present parallel and perpendicular $Pd_2(C_2H_2)$ isomers are analogous to the dimetallacyclobutene and quasi-tetrahedral structures in transition metal complex chemistry.[47−49]

When three Pd atoms (trimer) interact with C_2H_2, three isomers are obtained on the potential energy surface. The $(Pd_3)CCH_2$ vinylidene structure is the gobal minimum, the five-membered ring Pd_3−C_2H_2 structure is 20.3 kcal/mol higher, and a trigonal (CH)−Pd_3−(CH) isomer is 40.3 kcal/mol higher in energy. It is interesting to note the C−C bond in ring Pd_3−C_2H_2 is a double bond, but this bond is broken in (CH)−Pd_3−(CH) and the two C−H moieties are stabilized on both sides of the Pd_3 triangle. The $(Pd_3)CCH_2$ vinylidene structure is similar to the surface intermediate species, and the calculated C−C stretching frequencies are within 15 cm^{-1}.[12]

TABLE 4: Geometries and Frequencies Calculated at the B3LYP/6-311++G(d,p)/SDD Level of Theory for $Pd(C_2H_2)_{1,2}$ and $Pd_{2,3}(C_2H_2)$ Complexes

molecule	state	relative energy (kcal/mol)	geometries (Å, deg)	frequencies (cm^{-1}) (intensities, km/mol)
C_2H_2	$^1\Sigma_g^+$		CC, 1.209; CH, 1.070	3523.3(σ_g,0), 3420.6(σ_u,94), 2061.8(σ_g,0), 772.7(π_u,112 × 2), 647.5(π_g,0 × 2)
Pd-η^2-C_2H_2 (C_{2v})	$^1A_1$		PdC, 2.071; CC, 1.251; CH, 1.072; CPdC, 35.1; CCH, 156.8	3377.4(a_1,6), 3309.3(b_2,37), 1797.8(a_1,28), 768.9(b_2,81), 760.5(a_1,1), 705.6(b_1,86), 662.2(a_2,0), 412.6(a_1,10), 362.1(b_2,4)
Pd-η^2-$(C_2H_2)_2$ (D_{2d})	$^1A_1$		PdC, 2.094; CC, 1.245; CH, 1.071; CPdC, 34.6; CCH, 158.6	3390.2(a_1,0), 3390.2(b_2,28), 3319.8(e,41 × 2), 1832.4(b_2,125), 1821.5(a_1,0), 766.1(e,74 × 2), 759.4(?,0), 757.0(b_2,14), 738.4(e,33), 711.8(b_1,0), 705.5(a_2,0), 442.7(e,0 × 2), 415.4(b_2,39), 372.8(a_1,0), 219.5(b_1,0), 106.0(e,0 × 2)
parallel Pd_2-η^2-C_2H_2 (C_{2v})	$^1A_1$	0.0	PdC, 1.965; CC, 1.296; CH, 1.087; PdPd, 2.607; PdPdC, 70.5; CCH, 135.3	3165.7(a_1,0), 3127.3(b_2,1), 1623.1(a_1,53), 1001.0(b_2,48), 862.1(a_1,24), 667.5(a_2,0), 614.7(b_1,84), 550.8(a_1,10), 545.8(b_2,0), 268.0(b_2,0), 193.2(a_2,0), 176.3(a_1,0)
perpendicular Pd_2-η^2-C_2H_2 (C_{2v})	$^1A_1$	6.3	PdC, 2.091; CC, 1.308; CH, 1.077; PdPd, 2.852; CPdC, 36.4; PdCH, 128.2	3282.5(a_1,4), 3238.0(b_2,17), 1553.7(a_1,22), 838.1(b_2,101), 771.7(a_1,1), 720.6(b_1,3), 706.2(a_2,0), 397.3(b_2,11), 390.5(a_1,6), 382.2(b_1,7), 246.0(a_2,0), 106.3(a_1,0)
ring $Pd_3-(C_2H_2)$ (C_{2v})	$^1A_1$	0.0	Pd′C, 1.931; CC, 1.304; CH, 1.097; Pd′Pd″, 2.564; Pd′Pd″Pd′, 87.4; Pd′CC, 125.4; CCH, 127.8	3061.2(a_1,3), 3027.2(b_2,1), 1623.1(a_1,51), 1060.1(b_2,14), 902.7(a_1,26), 643.6(a_2,0), 575.2(b_2,3), 549.4(b_2,3), 510.1(a_1,0), 334.3(b_2,0), 201.6(a_2,0), 188.2(a_1,0), 186.5(a_1,0), 71.4(a_1,1), 30.9(b_1,0)
(CH)-Pd_3-(CH) (D_{3h})	$^1A_1$	33.4	PdC, 1.994; CH, 1.094; PdPd, 2.882	3073.0(0), 3065.9(0), 876.6(0), 876.3(1), 663.2(0), 662.4(0), 662.1(0), 519.1(0), 518.2(0), 507.9(38), 443.3(0), 194.8(0), 111.9(0), 111.1(0)

Hence, with increasing numbers of Pd atoms, the vinylidine isomer becomes more stable relative to the π complex.

BPW91 calculations were also performed on the related PdCCH species, which is a potential product of the reaction between Pd and CCH radical in these experiments, and the frequencies are similar to the results of an earlier B3LYP calculation.[50] We find $PdCCH^-$ to be 50 kcal/mol more stable than PdCCH, in good agreement with the 45.7 kcal/mol electron affinity.[50]

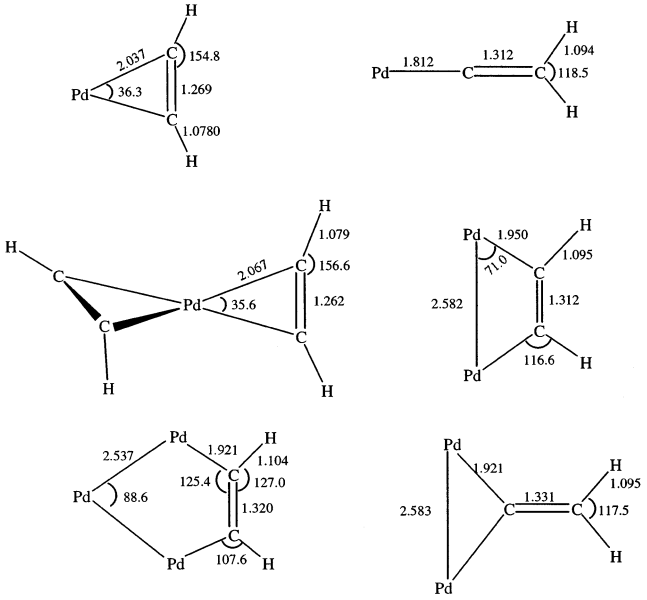

Figure 5. Structures calculated at the BPW91 level for palladium−acetylene complexes. Bond lengths are in Ångstroms, and bond angles are in degrees.

Discussion

Three new groups of absorptions will be assigned to Pd−C_2H_2 complexes based on frequency shifts with $^{13}C_2H_2$, C_2D_2, and C_2HD and DFT frequency calculations.

Pd-η^2-(C_2H_2). Group A bands are assigned to Pd-η^2-(C_2H_2). Weak 3163.8 and 3153.7 cm^{-1} absorptions, which are slightly lower than the C−H stretching mode for C_2H_2, are due to the b_2 C−H stretching vibration in this complex in two matrix sites. These bands shift to 3157.7 and 3147.4 cm^{-1} with $^{13}C_2H_2$ and give 1.0019 and 1.0020 isotopic frequency ratios. With C_2D_2, the C−D stretching mode appears at 2363.6 and 2360.2 cm^{-1} and defines a 1.337 ± 0.001 H/D ratio. A new band was observed at 3199.1 cm^{-1} with the mixed H,D−acetylene sample, but the C−D stretching region was masked by $(C_2D_2)_n$ species absorptions. The 1716.9, 1709.6, and 1707.1 cm^{-1} bands are due to matrix site-splitting for the C−C vibrational mode of this complex. These bands shift to 1659.1, 1651.8, and 1649.5 cm^{-1}, respectively, with $^{13}C_2H_2$, giving a 1.0349 $^{12}C/^{13}C$ isotopic frequency ratio. This mode is located in the C−C bond stretching region, but the deviation from the C−C harmonic ratio (1.0408) suggests that the C−C vibration is coupled to C−H motion in this molecule. The C−C stretching mode is active in this complex because the HCCH subunit is bent by interaction with the metal atom. In addition, the Pd($^{12}C^{13}CH_2$) molecule is observed at 1687.6, 1681.0, 1678.6 cm^{-1} from the 2% $^{12}C^{13}CH_2$ present in the $^{13}C_2H_2$ sample near the medians of pure isotopic bands. Further experiments with C_2D_2 confirm this mixed mode: the three bands shift to 1590.4, 1582.8, and 1579.4 cm^{-1}, respectively (Figure 2). With mixed H,D−acetylene (approximately 30% C_2H_2, 50% C_2HD, and 20% C_2D_2), the bands due to Pd-η^2-(C_2H_2), Pd-η^2-(C_2D_2) and new bands at 1649.7, 1641.6, and 1638.6 cm^{-1} appeared, in rough proportion to the precursor isotopic distribution (Figure 3). The latter are 4−5 cm^{-1} lower than the median

TABLE 5: Comparison of Calculated (BPW91) and Observed (Major Argon Matrix Site) Isotopic Frequencies (cm^{-1}) for Pd-η^2-(C_2H_2)

	obs	calcd	diff		obs	calcd	diff
$^{12}C_2H_2$	3163.8	3231.5 (b_2)	67.7	$^{12}C_2HD$	3199.1	3265.0	65.9
	1709.6	1720.7 (a_1)	11.1		1638.6	1646.7	8.1
	764.5	762.9 (b_2)	−1.6		757.5	764.4	6.9
	674.5	670.3 (b_1)	−4.2		653.8	637.0	−16.8
$^{13}C_2H_2$	3157.7	3222.2	64.5	$^{12}C_2D_2$	2363.6	2370.6	7.0
	1651.8	1661.6	9.8		1582.8	1583.9	1.1
	756.1	754.6	−1.5		635.7	619.7	−16.0
	671.5	667.3	−4.2		506.7	500.7	−6.0

of C_2H_2 and C_2D_2 product bands and must be assigned to Pd-η^2-(C_2HD).

Similar site-split bands at 769.6, 765.8, and 764.5 cm^{-1} track with the upper bands (Figure 1), shifting to 764.7, 757.3, and 756.1 cm^{-1} upon ^{13}C substitution. This mode is a CCH deformation (in-plane) for the HCCH moiety in this molecule, which is 28 cm^{-1} higher than that of free C_2H_2 at 737 cm^{-1}. The deuterium counterpart for this mode shifts to 635.7 cm^{-1}. Another CCH deformation mode (out-of-plane) for this molecule is found at 675.4 and 674.5 cm^{-1}, which shows 3 and 167.3 cm^{-1} red shifts with ^{13}C and D substitution, respectively. With the $^{12}C_2H_2 + {}^{13}C_2H_2$ mixture, the modes exhibit only pure isotopic bands indicating that only one C_2H_2 subunit is coordinated to the Pd atom, a result in accord with the relative band absorbances using the mixed C_2H_2, C_2HD, and C_2D_2 precursor. Finally, the latter mixed precursor gives new bands at 757.5 and 653.8 cm^{-1} for deformation modes of Pd-η^2-(C_2HD).

Experiments with neon produce the same major product absorptions (Table 2). The major site of the C−H and C−C stretching modes and out-of-plane C−H deformation blue-shifted 8, 5, and 3 cm^{-1}, respectively, in neon relative to argon, which are reasonable for stable complexes that do not interact strongly with the matrix environment.[51] It is anticipated that the neon matrix observations more closely approximate the gaseous complex.

A laser-ablated Pd experiment with 0.2% C_2H_4 in argon gave C_2H_2 as a product (737 cm^{-1} band 30% of 949 cm^{-1} precursor), and annealing to 30 K produced the same sharp bands (A = 0.001−0.002) reported here for the three strongest Pd-η^2-(C_2H_2) fundamentals. Further annealing to 35 and 40 K produced much stronger 1527.0 and 1259.2 cm^{-1} absorptions for the Pd-η^2-(C_2H_4) complex.

DFT frequency calculations with the BPW91 functional for Pd-η^2-(C_2H_2) predict observable C−H stretching, C−C stretching, and CCH deformation modes at 3231.5, 1720.7, 762.9, and 670.3 cm^{-1} and isotopic frequencies, which closely match the experimental observations. Table 5 compares the calculated and observed isotopic frequencies (major site). First, the predicted C−C stretching frequency is only 11 cm^{-1} higher than the experimental value, and the computed $^{12}C/^{13}C$ and H/D frequency ratios for this mode are essentially the same as the observed values. Note that the calculated C−C stretching mode in Pd-η^2-(C_2H_2) has a significant coupling with the C−H mode, and this mode in Pd-η^2-(C_2HD) is predicted 5.6 cm^{-1} lower than the median of C_2H_2 and C_2H_2 bands, which reproduces the observation very well. Second, two deformation modes predicted at 762.9 cm^{-1} (in-plane) and 670.3 cm^{-1} (out-of-plane) are only 2−4 cm^{-1} lower than the experimental values. The in-plane mode shows larger ^{13}C and smaller D shifts than the out-of-plane mode, which indicates mixing with other in-plane modes. The calculation gives two strong deformation modes for Pd-η^2-(C_2HD) at 764.4 and 737.0 cm^{-1} just 6.9 cm^{-1} higher and 16.8 cm^{-1} lower than observed. Third, the symmetric and antisymmetric C−H stretching vibrations are calculated at 3294.2 (very weak) and 3231.5 cm^{-1} (strong), respectively, which is in good agreement with the antisymmetric mode observed at 3163.8 cm^{-1}. The 3199.1 cm^{-1} band observed for Pd-η^2-(C_2HD) is 36.3 cm^{-1} higher than the antisymmetric C−H mode for Pd-η^2-(C_2H_2), in agreement with the 33.5 cm^{-1} higher DFT prediction. For Pd-η^2-(C_2HD), the C−H mode is approximately the average of the symmetric and antisymmetric C−H modes for Pd-η^2-(C_2H_2). Fourth, the calculated infrared intensities are in reasonable agreement with the observed band absorbances (approximately 0.005, 0.026, 0.041, and 0.063, respectively, in Figure 1b) although site splittings make quantitative measurement difficult. The strongest absorptions are CCH deformation modes, but the C−C stretch is relatively stronger and the C−H stretch relatively weaker than predicted by DFT. Frequencies calculated with the B3LYP functional are slightly higher (Table 3) as expected.[51]

Pd-η^2-(C_2H_2)$_2$. The Group B bands at 3184.2, 1765.3, 1762.9, 1760.4, 772.8, 769.6, and 710.1 cm^{-1} are favored at higher C_2H_2 concentrations and on annealing, and these bands are assigned to Pd-η^2-(C_2H_2)$_2$ and labeled PdA_2 in the figures. All of these absorptions are slightly higher than the bands due to Pd-η^2-(C_2H_2), and they exhibit similar ^{13}C and deuterium isotopic shifts. Accordingly, site-split bands at 1765.3, 1762.9, and 1760.4 cm^{-1} are assigned to the out-of-phase C−C stretching mode. There are four important features to note regarding this C−C stretching mode. The first is that this band is barely observed on deposition but increased greatly on annealing. The second is that this mode is strongly coupled by C−H vibration: it shifts to 1618.7 cm^{-1} with C_2D_2, which is analogous to Pd-η^2-(C_2H_2). The third is that with mixed H,D−acetylene, annealing produces bands at 1761.1 and 1618.4, which are 0.7 cm^{-1} above the lowest site-split component for the pure isotopic species, plus a stronger new band at 1683.3 cm^{-1}, which is 6.4 cm^{-1} below the median of the above pure isotopic absorptions. This latter band belongs to the C−C mode for C_2HD in a bis complex. The fourth is that the mixed $^{12}C_2H_2 + {}^{13}C_2H_2$ experiment gives major bands at 1760.9 and 1701.3 cm^{-1} for this species without the amount of site splitting observed in Figures 1 and 2. Hence, the mixed isotopic experiments only slightly affect the spectra of Pd-η^2-(C_2H_2)$_2$ complexes, and there is very little coupling between the two C_2H_2 moieties. In contrast, the matrix site structure for the Pd-η^2-(C_2H_2) complexes is not altered with the isotopic mixtures.

The in-plane deformation mode with site-split bands at 772.8 and 769.6 cm^{-1} and out-of-plane mode at 710.1 cm^{-1} show the same isotopic character as discussed for Pd-η^2-(C_2H_2). Unfortunately, the mixed isotopic distribution is indistinct for these modes because of band overlapping and broadening.

Excellent agreement is found between the DFT calculations and the observations for Pd-η^2-(C_2H_2)$_2$. Using the BPW91 functional, the b_2 C−C stretching mode is predicted at 1760.7 cm^{-1} with strong intensity, which is only 4.6 cm^{-1} below the experimental value, and the unobserved a_1 mode is predicted at 1746.3 cm^{-1} with zero intensity. The predicted deformation modes at 713.3 and 750.9 cm^{-1} and C−H stretching mode at 3242.6 cm^{-1} are within 3, 22, and 58 cm^{-1}, respectively, of the observed values.

The neon matrix has no effect on the out-of-phase C−C stretching mode, and it blue shifts the C−H stretch and strongest deformation mode 4 and 2 cm^{-1}, respectively, from argon matrix values. It can be rationalized that two C_2H_2 ligands insulate

the Pd center from matrix interaction more effectively than one C_2H_2 ligand.

Pd_2-η^2-(C_2H_2). A weak band with site-split components at 1572.3 and 1565.8 cm^{-1} appears on annealing over very weak common bands at 1577.0 and 1572.8 cm^{-1}, which falls in the C−C double bond stretching region. With $^{13}C_2H_2$, the bands shift to 1521.4 and 1515.6 cm^{-1}, and mixed $^{12}C_2H_2 + {}^{13}C_2H_2$ experiments give a sharp doublet indicating one C−C subunit in this molecule ($^{12}C/^{13}C$ ratios 1.0335, 1.0331). In our C_2D_2 experiments, these bands shift to 1506.4 and 1500.7 cm^{-1}, which is expected for a C−C stretching mode strongly perturbed by hydrogen. Again, three sharp band sets are observed with C_2H_2, C_2HD, and C_2D_2 and the new 1544.4, 1538.9 cm^{-1} intermediate pair is 5.1 and 5.6 cm^{-1} higher than the median for C_2H_2 and C_2D_2, which is similar to that found for the C−C stretching mode in the Pd-η^2-$(C_2H_2)_{1,2}$ complexes. Weaker matching site-split bands at 989.6, 985.7 cm^{-1} also track with these bands and shift to 975.5, 971.6 cm^{-1} with $^{13}C_2H_2$ and to 846.3, 844.7 cm^{-1} with C_2D_2. The 1.0145 $^{12}C/^{13}C$ ratio defines an in-plane H−CC−H deformation mode with considerable carbon motion. The H,D−acetylene experiment produces a new intermediate band set at 949.3, 945.7 cm^{-1}, this time higher by 31.0, 30.5 cm^{-1} than the median of pure isotopic band sets. Such asymmetry is characteristic of an antisymmetric mode (b_2) that changes form on symmetry lowering. These bands are favored relative to Pd(C_2H_2) when the Pd/C_2H_2 ratio is increased. Hence, we conclude that two Pd atoms coordinate to C_2H_2 and further reduce the C−C bond. Accordingly, the Pd_2-η^2-(C_2H_2) molecule is proposed.

The parallelogram Pd_2-η^2-(C_2H_2) structure is predicted to be a stable complex by DFT calculations, and the C−C stretching mode for parallel Pd_2-η^2-(C_2H_2) is 1563.6 cm^{-1} with the BPW91 functional, only 2−9 cm^{-1} lower than the observed value. The computed b_2 deformation mode at 986.6 cm^{-1} matches the experimental measurement. Note that the calculated C−C stretching mode in perpendicular Pd_2-η^2-(C_2H_2) is 100 cm^{-1} lower, and furthermore, this molecule is 5.0 kcal/mol higher in energy. We have no evidence for the slightly more stable $(Pd_2)CCH_2$ vinylidene structure or any vinylidene species expected to absorb in the 1400−1600 region.[10−13] The Pd_2-η^2-(C_2H_2) complex appears on annealing in solid argon where insufficient activation energy is available for rearrangement. The observation of the dimetallacyclobutene form rather than the quasitetrahedral isomer is in contrast to typical findings in transition metal complex chemistry.[47−49] Finally, the present parallelogram Pd_2-η^2-(C_2H_2) structure observed here is analogous to low-temperature chemisorbed acetylene, but a stronger interaction, and lower 1402 cm^{-1} frequency, is found for the surface species.[10]

Other Absorptions. Weak bands at 1987.7, 1899.0, and 1878.0 cm^{-1} exhibit slightly different behavior on annealing and photolysis: (i) the 1987.7 cm^{-1} peak increases on 35 K annealing, decreases on photolysis, and then restores on 35 K annealing and (ii) the 1899.0 and 1878.0 cm^{-1} absorptions increase slightly on 30 K annealing and disappear on photolysis. These peaks all show $^{13}C_2H_2$ and C_2D_2 shifts (Table 1) like CCH at 1845.8 cm^{-1}, which indicates a C−C stretching mode coupled to hydrogen. Furthermore, these bands were observed as sharp doublets in the $^{12}C_2H_2 + {}^{13}C_2H_2$ experiment, which shows that a single acetylene molecule is involved.

Our BPW91 calculations have proven accurate for the prediction of product absorptions in this system, and on this basis, the above sharp absorptions are assigned to PdCCH, isolated $PdCCH^-$, and perturbed $PdCCH^-$, respectively. The strong C−C stretching modes are predicted at 2014.7 and 1912.9 cm^{-1} for PdCCH and $PdCCH^-$, respectively, just 27.0 and 13.9 or 34.9 cm^{-1} higher than observed. Other weaker modes that might be observed fall in congested regions of the spectrum and are not detected. These PdCCH species are probably formed by direct Pd atom reactions with CCH radical, or CCH^- anion, all of which are produced by the laser ablation process. Our C≡C frequency for PdCCH is substantially higher than assigned[50] from a weak fine structure band in the photoelectron spectrum of $PdCCH^-$. The insertion of energetic Pd into the C−H bond of C_2H_2 to form HPdCCH with subsequent dissociation to PdH and CCH and to PdCCH may also occur in the laser ablation process.

A sharp, weak 1660.9 cm^{-1} absorption appeared on deposition of laser-ablated Pd with C_2H_2, decreased 50% on $\lambda > 240$ nm irradiation, and increased 20% on final 35 K annealing (Figure 1). This band shifted to 1601.6 cm^{-1} with $^{13}C_2H_2$ (1.0370 ratio) and is primarily a C−C stretching mode. A sharp doublet with the $^{12}C_2H_2 + {}^{13}C_2H_2$ mixture suggests a single acetylene product. The ^{13}C and D shifts are comparable to those observed for species A, and we believe that the weak 1660.9 cm^{-1} band is probably due to Pd-η^2-(C_2H_2) perturbed by another molecule in the matrix.

Bonding Considerations. The bonding of Pd atom with C_2H_2 is quite similar to the side-bonded $Pd(H_2)_{1,2,3}$ complexes; however, calculations at the BPW91 level give more exothermic reactions for Pd + C_2H_2 (1 and 2) than reactions of Pd + H_2 (3 and 4). Although Pd can complex three dihydrogen molecules in a trigonal planar complex,[5] there no evidence for three acetylene ligands. This contrasts Ni^+ where $Ni(C_2H_2)_3^+$ is the most stable ion cluster.[52]

$$Pd(^1S) + C_2H_2(^1\Sigma_g^+) \rightarrow Pd\text{-}\eta^2\text{-}(C_2H_2)(^1A_1) \quad \Delta E = -39.8 \text{ kcal/mol} \quad (1)$$

$$Pd\text{-}\eta^2\text{-}(C_2H_2)(^1A_1) + C_2H_2(^1\Sigma_g^+) \rightarrow Pd\text{-}\eta^2\text{-}(C_2H_2)_2(^1A_1) \quad \Delta E = -38.6 \text{ kcal/mol} \quad (2)$$

$$Pd(^1S) + H_2 \rightarrow Pd(H_2)(^1A_1) \quad \Delta E = -29.3 \text{ kcal/mol} \quad (3)$$

$$Pd(H_2)(^1A_1) + H_2 \rightarrow Pd(H_2)_2(^1A_1) \quad \Delta E = -26.3 \text{ kcal/mol} \quad (4)$$

The η^2 attachment of H_2 or C_2H_2 to atomic Pd can be understood by the simple model employed for bonding CO to transition metals.[3] Palladium ground state with the s^0d^{10} configuration is less reactive than the open shell s^1d^9 state (the Pt ground state cleaves the H−H bond without energy barrier).[9a,16a] Atomic Pd provides an empty s orbital to receive electron donation from σ or π molecular orbitals of H_2 or C_2H_2 and d orbital back donation to σ^* on H_2 or π^* on C_2H_2. Comparing the natural electron configurations of $Pd(H_2)$ and Pd-η^2-(C_2H_2) calculated from NBO analysis (Table 6),[33] the 5s population is higher and the 4d population is lower in Pd-η^2-(C_2H_2) than that in $Pd(H_2)$, indicating that both donation and back donation are more effective in Pd-η^2-(C_2H_2). A similar trend is found in Pd-η^2-$(C_2H_2)_2$ and $Pd(H_2)_2$. Accordingly, the C−C triple bond is weakened in side-bonded complexes.

We find no evidence for the higher energy $PdCCH_2$ vinylidene isomer, even on photolysis. Apparently, sufficient activation energy for this rearrangement is not available in our experiment. This is consistent with the surface observations that adsorbed acetylene is formed at lower temperature and that warming above 200 K is required for rearrangement to the

TABLE 6: Natural Electron Configurations and Atomic Charge Distributions for Palladium Complexes[a]

	Pd-η^2-H_2	Pd-η^2-$(H_2)_2$	C_2H_2	Pd-η^2-C_2H_2	Pd-η^2-$(C_2H_2)_2$	parallel Pd_2-η^2-C_2H_2	ring Pd_3-η^2-(C_2H_2)
Pd	[core]$5s^{0.24}4d^{9.71}$ 0.046[b] (0.053)[c]	[core]$5s^{0.47}4d^{9.62}$ −0.098 (0.046)		[core]$5s^{0.35}4d^{9.44}$ 0.203 (0.351)	[core]$5s^{0.52}4d^{9.50}$ 0.315 (0.844)	[core]$5s^{0.42}4d^{9.40}$ 0.178 (0.204)	[core]$5s^{0.47}4d^{9.33}$ 0.208 (0.313)[d]
C			[core]$2s^{1.03}2p^{3.19}$ −0.225 (−0.272)	[core]$2s^{1.07}2p^{3.24}$ −0.330 (−0.386)	[core]$2s^{1.06}2p^{3.24}$ −0.315 (−0.416)	[core]$2s^{1.09}2p^{3.27}$ −0.389 (−0.425)	[core]$2s^{1.10}2p^{3.26}$ −0.386 (−0.522)
H	$1s^{1.01}$ (−0.026)	$1s^{0.97}$ 0.024 (−0.011)	$1s^{0.77}$ 0.225 (0.272)	$1s^{0.77}$ 0.229 (0.211)	$1s^{0.76}$ 0.236 (0.205)	$1s^{0.79}$ 0.211 (0.220)	$1s^{0.79}$ 0.206 (0.227)

[a] Based on BPW91/6-311++G(dp)/SDD calculations. [b] Natural atomic charges. [c] Mulliken atomic charges in parentheses. [d] For unique center Pd atom: [core]$5s^{0.46}4d^{9.59}$, −0.055 (−0.034).

vinylidene intermediate.[10−13] The natural charges show that Pd transfers less charge to C_2H_2 in $PdCCH_2$ than in the π complex $Pd(C_2H_2)$. Furthermore, the Pd−C bond in $PdCCH_2$ is calculated to be a short, 1.812 Å, normal electron pair bond, but the Pd−C bond in $Pd(C_2H_2)$ is longer, 2.037 Å. The calculated C−C frequency for $PdCCH_2$, 1678.6 cm^{-1}, is slightly lower than the computed value for Pd-η^2-(C_2H_2), 1720.7 cm^{-1}.

As C_2H_2 is reacted with two Pd atoms (Pd dimer), the C−C triple bond is reduced to a double bond in a parallelogram Pd_2-η^2-(C_2H_2) complex based on our DFT calculations. The charge distributions clearly show that more electrons are transferred to the C−C bond from Pd_2 dimer (reaction 5). Recall the interaction of Pd_2 dimer with H_2 (reaction 6); the H−H bond is totally broken, which has been observed in low-temperature neon and argon matrices and reproduced very well from theoretical calculations.[5,9a]

$$Pd(^1S) + Pd\text{-}\eta^2\text{-}(C_2H_2)(^1A_1) \rightarrow Pd_2\text{-}\eta^2\text{-}(C_2H_2)(^1A_1) \qquad \Delta E = -46.7 \text{ kcal/mol} \quad (5)$$

$$Pd(^1S) + Pd(H_2)(^1A_1) \rightarrow (PdH)_2(^1A_g) \qquad \Delta E = -53.3 \text{ kcal/mol} \quad (6)$$

A relevant bonding comparison is the effect of Pd on C_2H_4 in a similar π complex. This complex has been identified at 1502 and 1223 cm^{-1} in solid xenon,[53] and these coupled CH_2 bending and C=C stretching modes both involve the diagnostic double bond. A detailed study with Ni revealed 1468.2 and 1165.9 cm^{-1} argon matrix fundamentals for Ni-η^2-(C_2H_4), and the lower mode exhibited twice the $^{13}C_2H_4$ shift as the upper mode.[54] Our laser ablation experiment with Pd and C_2H_4 in argon gave major bands at 1527.0 and 1259.2 cm^{-1}, which show that Ni interacts more strongly with C_2H_4 than Pd (the C=C mode of C_2H_4 is 1623.3 cm^{-1}).[55] Likewise, Ni displaces the C_2H_2 fundamental (to 1634.8 cm^{-1})[23] more than Pd in the η^2 complexes. It appears that Pd has a comparable effect in reducing the π bonding in C_2H_2 and C_2H_4.

Conclusions

Reactions of laser-ablated palladium atoms with acetylene in excess argon produced Pd-η^2-(C_2H_2), Pd-η^2-$(C_2H_2)_2$, and parallel Pd_2-η^2-(C_2H_2) complexes, which are identified by isotopic shifts ($^{13}C_2H_2$, C_2D_2, C_2HD) and DFT (BPW91 and B3LYP functional) calculations. Pd-η^2-(C_2H_2) gives a major C−C stretching vibration at 1709.6 cm^{-1}, C−H stretching modes at 3163.8 and 3153.7 cm^{-1}, and C−H deformation modes at 764.5 and 675.4 cm^{-1}. Pd-η^2-$(C_2H_2)_2$, which is favored at higher C_2H_2 concentration and increased on annealing and photolysis, produced a C−C stretching mode at 1765.3 cm^{-1}. Additional absorptions at 1572.3 and 1565.8 cm^{-1} are due to the C−C stretching vibration in the Pd_2-η^2-(C_2H_2) complex, where Pd_2 dimer parallel coordinates C_2H_2, and the C−C triple bond is reduced to a double bond. This Pd_2-η^2-(C_2H_2) molecule is analogous to chemisorbed acetylene.[10] These absorptions show small 3−8 cm^{-1} shifts in neon, which characterize weak matrix interactions. Excellent agreement with DFT isotopic frequency calculations substantiates identification of these strong palladium−acetylene complexes.

Acknowledgment. We gratefully acknowledge support for this work from N.S.F. Grant CHE 00-78836

References and Notes

(1) Negishi, E. I.; Copéret, C.; Ma, S.; Liou, M.-Y.; Liu, F. *Chem. Rev.* **1996**, *96*, 365.
(2) Dedieu, A. *Chem. Rev.* **2000**, *100*, 543.
(3) Liang, B.; Zhou, M. F.; Andrews, L. *J. Phys. Chem. A* **2000**, *104*, 3905.
(4) (a) Carroll, J. J.; Haug, K. L.; Weisshaar, J. C. *J. Am. Chem. Soc.* **1993**, *115*, 6962. (b) Holthausen, M. C.; Koch, W. *J. Am. Chem. Soc.* **1996**, *118*, 9932. (c) Wen, Y.; Porembski, M.; Ferrett, T. A.; Weisshaar, J. C. *J. Phys. Chem. A* **1998**, *102*, 8362. (d) Willis, P. A.; Stauffer, H. U.; Hinrichs, R. Z.; Davis, H. F. *J. Phys. Chem. A* **1999**, *103*, 3706.
(5) (a) Andrews, L.; Manceron, L.; Alikhani, M. E.; Wang, X. *J. Am. Chem. Soc.* **2000**, *122*, 11011. (b) Andrews, L.; Wang, X.; Alikhani, M. E.; Manceron, L. *J. Phys. Chem. A* **2001**, *105*, 3052 (Pd + H_2).
(6) Balasubramanian, K. *J. Chem. Phys.* **1988**, *89*, 6310.
(7) (a) Blomberg, M. R. A.; Siegbahn, P. E. M. *Chem. Phys. Lett.* **1991**, *179*, 524. (b) Blomberg, M. R. A.; Siegbahn, P. E. M.; Svensson, M. *J. Phys. Chem.* **1992**, *96*, 5783.
(8) Castillo, S.; Cruz, A.; Bertin, V.; Poulain, E.; Arellano, J. S.; Del Angel, G. *Intl. J. Quantum Chem.* **1997**, *62*, 29.
(9) (a) Cui, Q.; Musaev, D. G.; Morokuma, K. *J. Chem. Phys.* **1998**, *108*, 8418. (b) Moc, J.; Musaev, D. G.; Morokuma, K. *J. Phys. Chem. A* **2000**, *104*, 11606.
(10) (a) Gates, J. A.; Kesmodel, L. L. *J. Chem. Phys.* **1982**, *76*, 4281. (b) Gates, J. A.; Kesmodel, L. L. *Surf. Sci.* **1983**, *123*, 68.
(11) Ormerod, R. M.; Lambert, R. M.; Hoffmann, H.; Zaera, F.; Wang, L. P.; Bennett, D. W.; Tysoe, W. T. *J. Phys. Chem.* **1994**, *98*, 2134.
(12) Clotet, A.; Ricart, J. M.; Pacchioni, G. *J. Mol. Struct. (THEOCHEM)* **1999**, *458*, 123.
(13) (a) Azad, S.; Kaltchev, M.; Stacchiola, D.; Wu, G.; Tysoe, W. T. *J. Phys. Chem. B* **2000**, *104*, 3107. (b) Jungwirthová, I.; Kesmodel, L. L. *J. Phys. Chem. B* **2001**, *105*, 674.
(14) (a) Wang, X.; Andrews, L. *J. Am. Chem. Soc.* **2001**, *123*, 12899. (b) Wang, X.; Andrews, L. *J. Phys. Chem. A* **2002**, *106*, 3744 (Au + H_2).
(15) (a) Wang, X.; Andrews, L. *J. Phys. Chem. A* **2002**, *106*, 3706 (Rh + H_2). (b) Wang, X.; Andrews, L. *J. Am. Chem. Soc.* **2002**, *124*, 7610 (Sc, Y, La + H_2).
(16) (a) Andrews, L.; Wang, X.; Manceron, L. *J. Chem. Phys.* **2001**, *114*, 1559 (Pt + H_2). (b) Wang, X.; Andrews, L. *J. Am. Chem. Soc.* **2002**, *124*, 5636 (WH_6).
(17) Manceron, L.; Andrews, L. *J. Am. Chem. Soc.* **1985**, *107*, 563 (Li + C_2H_2).
(18) (a) Kasai, P. H. *J. Phys. Chem.* **1982**, *86*, 4092. (b) Kasai, P. H. *J. Am. Chem. Soc.* **1992**, *114*, 3299 (Na + C_2H_2).
(19) Thompson, C. A.; Andrews, L. *J. Am. Chem. Soc.* **1996**, *118*, 10242 (Be, Mg + C_2H_2).
(20) (a) Bopegedera, A. M. R. P.; Brazier, C. R.; Bernath, P. F. *Chem. Phys. Lett.* **1987**, *136*, 97. (b) Whitham, C. J.; Seop, B.; Visticot, J. P.; Keller, A. *J. Chem. Phys.* **1990**, *93*, 991.

(21) (a) Martin, J. M. L.; Taylor, P. R.; Hassanzadeh, P.; Andrews, L. *J. Am. Chem. Soc.* **1993**, *115*, 2510. (b) Andrews, L.; Hassanzadeh, P.; Martin, J. M. L.; Taylor, P. R. *J. Phys. Chem.* **1993**, *97*, 5839 (B + C_2H_2). (c) Burkholder, T. R.; Andrews, L. *Inorg. Chem.* **1993**, *32*, 2491 (Al, Ga, In + C_2H_2). (d) Chertihin, G. V.; Andrews, L.; Taylor, P. R. *J. Am. Chem. Soc.* **1994**, *116*, 3513 (Al + C_2H_2).

(22) Kline, E. S.; Kafafi, Z. H.; Hauge, R. H.; Margrave, J. L. *J. Am. Chem. Soc*. **1985**, 107, 7559 (Fe + C_2H_2).

(23) Kline, E. S.; Kafafi, Z. H.; Hauge, R. H.; Margrave, J. L. *J. Am. Chem. Soc*. **1987**, *109*, 2402 (Ni + C_2H_2).

(24) Chatt, J.; Guy, R. G.; Duncanson, L. A. *J. Chem. Soc.* **1961**, 827.

(25) Greaves, E. O.; Lock, C. J. L.; Maitlis, P. M. *Can. J. Chem.* **1968**, *46*, 3879.

(26) Chatt, J.; Rowe, G. A.; Williams, A. A. *Proc. Chem. Soc*. **1957**, 208.

(27) (a) Burkholder, T. R.; Andrews, L. *J. Chem. Phys.* **1991**, *95*, 8697. (b) Bare, W. D.; Citra, A.; Chertihin, G. V.; Andrews, L. *J. Phys. Chem. A* **1999**, *103*, 5456.

(28) Frisch, M. J.; Trucks, G. W.; Schlegel, H. B.; Scuseria, G. E.; Robb, M. A.; Cheeseman, J. R.; Zakrzewski, V. G.; Montgomery, J. A., Jr.; Stratmann, R. E.; Burant, J. C.; Dapprich, S.; Millam, J. M.; Daniels, A. D.; Kudin, K. N.; Strain, M. C.; Farkas, O.; Tomasi, J.; Barone, V.; Cossi, M.; Cammi, R.; Mennucci, B.; Pomelli, C.; Adamo, C.; Clifford, S.; Ochterski, J.; Petersson, G. A.; Ayala, P. Y.; Cui, Q.; Morokuma, K.; Malick, D. K.; Rabuck, A. D.; Raghavachari, K.; Foresman, J. B.; Cioslowski, J.; Ortiz, J. V.; Stefanov, B. B.; Liu, G.; Liashenko, A.; Piskorz, P.; Komaromi, I.; Gomperts, R.; Martin, R. L.; Fox, D. J.; Keith, T.; Al-Laham, M. A.; Peng, C. Y.; Nanayakkara, A.; Gonzalez, C.; Challacombe, M.; Gill, P. M. W.; Johnson, B. G.; Chen, W.; Wong, M. W.; Andres, J. L.; Head-Gordon, M.; Replogle, E. S.; Pople, J. A. *Gaussian 98*, revision A.6; Gaussian, Inc.: Pittsburgh, PA, 1998.

(29) (a) Becke, A. D. *J. Chem. Phys.* **1993**, *98*, 5648. (b) Lee, C.; Yang, W.; Parr, R. G. *Phys. Rev. B* **1988**, *37*, 785.

(30) (a) Becke, A. D. *Phys. Rev. A* **1988**, *38*, 3098. (b) Perdew, J. P.; Wang, Y. *Phys. Rev. B* **1992**, *45*, 13244.

(31) (a) Krishnan, R.; Binkley, J. S.; Seeger, R.; Pople, J. A. *J. Chem. Phys.* **1980**, *72*, 650. (b) Frisch, M. J.; Pople, J. A.; Binkley, J. S. *J. Chem. Phys.* **1984**, *80*, 3265.

(32) Andrae, D.; Haussermann, U.; Dolg, M.; Stoll, H.; Preuss, H. *Theor. Chim. Acta* **1990**, *77*, 123.

(33) Reed, A. E.; Curtiss, L. A.; Weinhold, F. *Chem. Rev.* **1988**, *88*, 899.

(34) Andrews, L.; Kushto, G. P.; Zhou, M.; Willson, S. P.; Souter, P. F. *J. Chem. Phys.* **1999**, *110*, 4457.

(35) Forney, D.; Jacox, M. E.; Thompson, W. E. *J. Mol. Spectrosc*. **1995**, *170*, 178.

(36) Jacox, M. E. *J. Phys. Chem. Ref. Data* **1994**, *3*, 32 and references therein.

(37) Shen, L. N.; Doyle, T. J.; Graham, W. R. M. *J. Chem. Phys.* **1990**, *93*, 1597. These workers also assign a 2083.9 cm^{-1} band to C_4H, but in our experiments, this band varies from 20 to 80% of the 2060.4 cm^{-1} band intensity.

(38) Patten, K. O.; Andrews, L. *J. Phys. Chem.* **1986**, *90*, 3910.

(39) Moore, C. B.; Pimentel, G. C. *J. Chem. Phys.* **1963**, *38*, 2816.

(40) Shen, L. N.; Graham, W. R. M. *J. Chem. Phys.* **1989**, *91*, 5115 (C_4). The $^{13}C_4$ isotopic molecule was not reported; however, $^{13}C_4$ is observed at 1483.6 cm^{-1} in our $^{13}C_2H_2$ experiments. See ref 36 for neon matrix counterpart.

(41) (a) Klotzbucher, W.; Ozin, G. A. *J. Am. Chem. Soc.* **1975**, *97*, 2672. (b) Wang, X.; Andrews, L.; Manceron, L. Unpublished work (Pd + N_2).

(42) Tremblay, B.; Manceron, L. *Chem. Phys.* **1999**, *250*, 187.

(43) Shepherd, R. A.; Doyle, T. J.; Graham, W. R. M. *J. Chem. Phys.* **1988**, *89*, 2738 (C_2H_3).

(44) Andrews, L.; Johnson, G. L.; Kelsall, B. J. *J. Chem. Phys.* **1982**, *76*, 5767 (C_2H_4).

(45) Siegbahn, P. E. M. *Theor. Chim. Acta* **1994**, *87*, 277.

(46) Sodupe, M.; Bauschlicher, C. W., Jr. *J. Phys. Chem.* **1991**, *95*, 8640.

(47) Cotton, F. A.; Jamerson, J. D.; Stults, B. R. *J. Am. Chem. Soc.* **1976**, *98*, 1774.

(48) Muetterties, E. L.; Pretzer, W. R.; Thomas, M. G.; Beier, B. F.; Thorn, D. L.; Day, V. W.; Anderson, A. B. *J. Am. Chem. Soc.* **1978**, *100*, 2090.

(49) (a) Wang, Y.; Coppens, P. *Inorg. Chem.* **1976**, *15*, 1122. (b) Thorn, D. L.; Hoffmann, R. *Inorg. Chem.* **1978**, *17*, 126.

(50) Moravec, V. D.; Jarrold, C. C. *J. Chem. Phys.* **2000**, *112*, 792.

(51) Zhou, M. F.; Andrews, L.; Bauschlicher, C. W., Jr. *Chem. Rev.* **2001**, *101*, 1931.

(52) Walters, R. S.; Jaeger, T. D.; Duncan, M. A. *J. Phys. Chem. A* **2002**, *106*, 10482.

(53) Ozin, G. A.; Power, W. J. *Inorg. Chem.* **1977**, *16*, 212.

(54) Lee, Y. K.; Hannachi, Y.; Xu, C.; Andrews, L.; Manceron, L. *J. Phys. Chem.* **1996**, *100*, 11228.

(55) Herzberg, G. *Infrared and Raman Spectra of Polyatomic Molecules*; D. Van Nostrand: New York, 1945.